Computed myography (CMG): Three dimensional reconstruction of motor functions from surface EMG data

Kees van den Doel[1], Uri M. Ascher[1], Armin Curt[2], John Steeves[2], and Dinesh K. Pai[1]

***Abstract*— We describe a methodology to qualitatively and quantitatively determine the activation level of individual muscles by voltage measurements from an array of voltage sensors on the skin surface. A physical finite element model for electrostatics simulation is constructed from morphometric data and numerical inversion techniques are used to determine muscle activation patterns. Preliminary results from experiments with simulated and human data are presented for activation reconstructions of three muscles in the upper arm (biceps brachii, bracialis, and triceps). This approach potentially offers a new clinical tool to sensitively assess muscle function in patients suffering from neurological disorders (e.g., spinal cord injury) and could more accurately guide advances in the evaluation of specific rehabilitation training regimens.**

I. Introduction

The recovery of motor (muscle paresis) and movement (trajectory) function in patients suffering from a disorder/damage within the peripheral and/or central nervous system is one of the key goals of medical and rehabilitative treatments, but accurate measurement of any change in recovery is less than optimal (i.e., sensitive or accurate). The conventional neurological examination of upper limb motor deficit in patients suffering from a cervical spinal cord injury, resulting in a tetraplegia, serves the purpose to: 1) diagnose the extent of neurogenic muscle paralysis, and 2) monitor changes over time after injury during rehabilitation. However, the underlying neurophysiological mechanisms cannot be inferred by these clinical assessments and subsequently clinical monitoring is restricted to describing a general pattern of recovery [1].

The general aim of the methods described here is to provide a detailed mapping of the activity of individual muscles by using surface electromyography (sEMG) data from multiple recording sites. This has direct applications for the clinical monitoring of functional recovery and the evaluation of specific rehabilitation programs for the improvement of muscle function in patients suffering from spinal cord injury.

Advances in computer hardware and software now permit the accurate simulation of electrical signal propagation in complex three dimensional geometries such as human limbs. The sources of electrical signals originating from muscle fibers are relatively well understood; both simple and detailed models for these are available, see [2]. For example in [3] a multi-layer finite element model (FEM) of an idealized cylindrical limb was used to predict the sEMG signal detected when a single source is present. We shall refer to this type of model as a *forward model*.

Our goal is to invert this procedure and reconstruct current sources, inside muscles of a limb, using simultaneous spatial information from a surface-mounted grid of sEMG sensors. The reconstructed sources are such that the measured sEMG data will be explained by the model. A model that predicts sources from data is called an *inverse model*. This inverse problem, in its general form, is well known [4] to have no unique solution, i.e., many different sources can fit the data precisely. We therefore need to constrain the solution to the inverse problem, and we do this by introducing a priori information. We call the resulting system CMG, for Computed Myography.

The only previous work [5], [6], [7], [8] on source localization in sEMG that we are aware of uses an overdetermined discrete source model, whereas we use an underdetermined distributed source model. No significant results against which to compare our work with appeared in these papers.

Clinical applications of high density sEMG were reviewed in [9]. These applications focus mainly on measuring detailed properties such as pulse shape of individual motor unit action potentials utilizing multiple surface electrodes as an alternative to needle EMG, and not on a comprehensive mapping of the current sources within a muscle (i.e., localization). These methods require similar measurement techniques as our method, i.e., a grid of simultaneous sensors, whereas the data analysis has no overlap with our method. See for example the HD-sEMG hardware described in [10].

Temporal information can be used to attempt to separate the mixing of signals from multiple motor units ("crosstalk") in sEMG. With advanced processing methods such as "precision decomposition" [11] it is possible to separate up to 5 motor units. In many applications crosstalk elimination (or reduction) is a central challenge, see for example [12], [11]. However for our purposes crosstalk is not a problem, but rather part of the solution as it is precisely the mixing of signals from different locations in individual voltage sensors that enables the reconstruction of spatial information of the various current sources in the muscles.

Activity source localization within the brain, from surface electroencephalogram (EEG) data, has been an active area of research for decades. A recent review of the state of the art of EEG inverse modeling can be found in [13]. The sEMG inverse problem has many similarities to the EEG inverse problem and our method is closely related to the LORETA system described in [13], [14].

[1]Dept. of Computer Science, University of British Columbia, Canada.
[2]ICORD (International Collaboration on Repair Discoveries), University of British Columbia, Canada.

This work was supported in part by the Peter Wall Institute for Advanced Studies, Canada Research Chairs Program, NSERC, CFI, and BC KDF.

II. Inverse Modeling

Our source localization methodology consists of the following steps, illustrated in Fig. 1. 1) Acquire a three dimensional geometry model by the segmentation of MRI data. 2) Build a finite element model (FEM) simulator (a forward model) for 3D volume conduction which can predict surface voltages (e.g., data) from given current sources in the muscles. The electrostatic potential $u(\mathbf{x})$ satisfies the generalized Poisson partial differential equation on the domain Ω

$$-\boldsymbol{\nabla}(\boldsymbol{\sigma}\boldsymbol{\nabla})u = I(\mathbf{x}) \quad \text{in} \quad \Omega, \tag{1a}$$

$$\nabla_{\boldsymbol{n}}\boldsymbol{\sigma}u = 0 \quad \text{on} \quad \partial\Omega_1, \tag{1b}$$

$$\nabla_{\boldsymbol{n}}\boldsymbol{\sigma}u = -\Sigma u \quad \text{on} \quad \partial\Omega_2, \tag{1c}$$

where $\boldsymbol{n}$ is the outward normal at the boundary, $\boldsymbol{\sigma}(\mathbf{x})$ is the conductivity tensor, and the source $I(\mathbf{x})$ is the transmembrane current density, which we assume is proportional to the second spatial derivative along the muscle fiber direction of the muscle fiber intracellular action potential (IAP) $V(\boldsymbol{x}, t)$. We distinguish two types of boundaries, the physical boundary $\partial\Omega_1$, and the cut boundary $\partial\Omega_2$ which represents the boundary of our model (i.e., a cut through the arm). The Σ term is an effective resistance modeling the flow of currents in and out of our modeling domain at its artificial boundaries. We discretize (1) with the COMSOL Multiphysics FEM package and export the matrices of the resulting linear system to MATLAB. 3) Using an inverse model, compute (using MATLAB) the most likely current sources that can explain measured data. Such an inversion problem is typically ill-posed, which means that the solution is not unique and/or the solution depends discontinuously on the data. Regularization, incorporating a priori information, is then employed to incorporate our prior knowledge of the

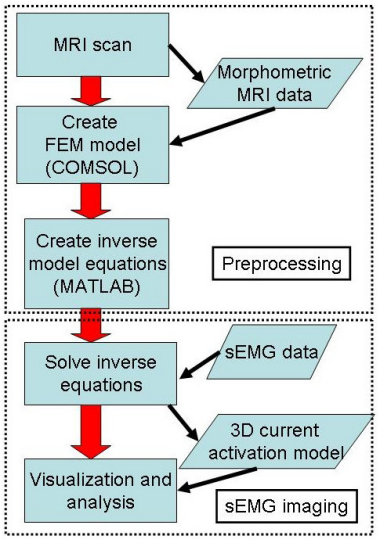

Fig. 1. Diagram of the CMG system. The thick arrows indicate sequential processing steps, the thin arrows indicate data produced or used, rectangles represent processes, and the slanted rectangles represent data. The preprocessing is done once for a patient, and remains valid as long as no significant change in morphology takes place.

electrical activities in the muscles which includes properties such as smoothness and the regions of possible activation. We then reconstruct the current sources $\boldsymbol{m}$ in the muscle fibers by minimizing the least square data fitting error plus a generalized Tikhonov regularization penalty function [15] that incorporates our a priori information. Denote our measured data by the vector $\boldsymbol{b}$. Define the linear operator $\boldsymbol{Q}$ which produces a vector of measurements from the potential field $u(\mathbf{x})$. The measurements can be monopolar, differential, or any other linear form. Note that $\boldsymbol{Q}$ also carries information about the reference electrode, when used. We are looking for a source that produces a potential field $u(\mathbf{x})$ such that $\boldsymbol{Q}u(\mathbf{x}) \approx \boldsymbol{b}$. Let us write $I(\mathbf{x}) = \boldsymbol{D}m(\mathbf{x})$ where m is the source function to be reconstructed. The operator $\boldsymbol{D}$ can be taken to be the identity, in which case m is just the current density I, or we can choose (assuming the muscle fibers are aligned in the z direction) $\boldsymbol{D} = \partial^2/\partial z^2$, in which case m is the transmembrane potential V. More complicated operators $\boldsymbol{D}$ based on known properties of the IAP are possible too. The inverse problem is then formulated as a constrained optimization problem

$$\min\ \phi(\boldsymbol{u}, \boldsymbol{m}) := \frac{1}{2}||\boldsymbol{Q}u - \boldsymbol{b}||^2 + \frac{1}{2}\int_\Omega m(\mathbf{x})\boldsymbol{Z}m(\mathbf{x})d\mathbf{x}, \tag{2}$$

$$\begin{aligned} &\text{subject to :} \\ &-\boldsymbol{\nabla}(\boldsymbol{\sigma}\boldsymbol{\nabla})u = \boldsymbol{m} \qquad \text{in } \Omega, \\ &\quad \nabla_{\boldsymbol{n}}\boldsymbol{\sigma}u = 0 \qquad \text{on } \partial\Omega_1, \\ &\quad \nabla_{\boldsymbol{n}}\boldsymbol{\sigma}u = -\Sigma u \quad \text{on } \partial\Omega_2, \end{aligned}$$

where the regularization operator $\boldsymbol{Z}$ is taken to be

$$\boldsymbol{Z} = -\beta(\boldsymbol{\nabla}(\boldsymbol{W}\boldsymbol{\nabla}) + \mu I) \tag{3}$$

with constants β and μ to be determined. The diagonal matrix $\boldsymbol{W}$, normalized to $\text{trace}(\boldsymbol{W}) = 3$, determines the anisotropy of the smoothing operator which we allow to have different values in the fiber direction and in the orthogonal directions. These parameters have different (constant) values on different anatomical regions. For example the "mass" μ is chosen to be very large outside muscle domains to force $\boldsymbol{m}$ to negligible values there. Inside a region of interest μ balances the cost of smoothness versus magnitude and for large values of μ we obtain the minimum norm solution. We determine good values for these constants empirically by reconstruction tests with known synthetic data and human data where we know the answer. The value of the overall scaling parameter β balances the relative weights given to the least-squares difference between predicted and measured data versus the a priori properties imposed on the solution. Extensive literature (see for example [16] for a review) exists on how to determine β in inverse problems. We use the Morozov discrepancy principle [16], which means we use a value of β so that the data is fitted to within measurement noise.

In Fig. 2 we show the anatomical image we used to build an upper arm model, a 3D geometry, and a tetrahedral mesh created on the geometry. Comparing the predicted and the

measured data we then calculate the current sources in the muscles, see Fig. 1.

The CMG system was implemented and tested on a desktop computer with a dual core 3GHz processor and 4Gb of RAM. Processing of sEMG data to produce the source estimations typically takes 15 minutes. The large sparse linear system of equations arising from the inversion algorithm was solved in MATLAB using a preconditioned conjugate gradient method with a preconditioner similar to the one described in [17]. The number of iterations required is typically about 50.

III. Results

In this section we describe results that have been obtained with the current prototype of the CMG software we have created.

We have constructed a model of the upper arm with three muscles (biceps, brachialis, and triceps, see Fig. 2) and tested the CMG system. Simulations with synthetic data indicate that activation of each of the three muscles can be derived accurately from sEMG data if a sufficiently dense (we used 215) surface grid of monopolar sensors is used. The experiments are summarized in Figs. 3, 4, and 5. In another set of experiments we obtained bipolar (differential) sEMG data from a healthy human subject during isometric flexion and extension using a ring of 12 bipolar sensors around the upper arm. A Delsys Bagnoli$^{\text{TM}}$ Desktop EMG Systems was used for the measurements. Differential sensors were employed since they are more widely used in sEMG than monopolar sensors, so it is important to determine if they can be used effectively with this method.

The sensors were placed approximately in the middle of the upper arm in the configuration depicted in Fig. 2. The subject was first asked to apply a constant force in the upper direction with the elbow at an angle of about 90^0. This is expected to activate the biceps and brachialis but not the triceps. Data was taken at $1000Hz$ for 15s. Second, the

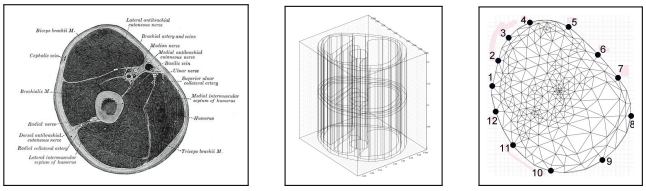

(a) Anatomical image (b) 3D geometry constructed (c) Mesh and 12 sensors

Fig. 2. A cross section of a generic upper arm (a) was used. The image was segmented into different anatomical regions: brachialis, biceps, triceps, fat and skin, and bone. The resulting 2D regions were then extruded in the vertical direction to create a 3D geometry (b) and imported in the finite element software COMSOL. The 3D geometry was then meshed with tetrahedral elements, and the inverse model equations were discretized in COMSOL and exported to MATLAB. We can then generate synthetic data, for example at the locations shown in the cross-sectional view of the mesh (c), placing known current sources in the muscles, or we can use measured data. After obtaining the sEMG data (synthetic or human) we then solve the inverse model equations in MATLAB and obtain reconstructed current sources in the muscles. We then import the result back into COMSOL for analysis and visualization.

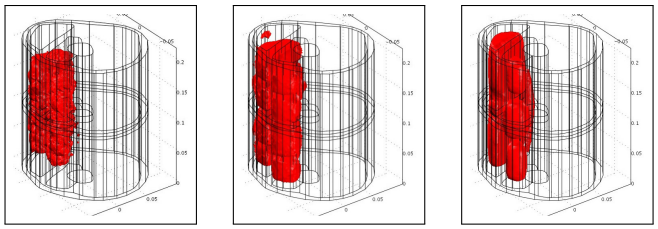

(a) Synthetic source model (b) Reconstructed model with surface data (215 points) (c) Reconstructed model with ring data (56 points)

Fig. 3. The CMG system was tested by creating simulated data. In the example shown here, we placed $5,000$ current tripole sources (displayed in (a)) at random locations in the biceps and brachialis. We visualize the region of activation by displaying a surface that encloses 80% of the current sources as measured by the integrated current power. We then compute synthetic monopolar sEMG data on a grid of 215 points distributed over the surface, and added 5% simulated Gaussian measurement noise. The current sources are then reconstructed from the surface data, see (b). We then discarded all surface data except for a ring of 56 points around the center of the arm and performed the inversion with this limited data, shown in (c). An objective measure of activation of the whole muscle is taken to be the current source power density, which is the same (by construction) in both muscles in the synthetic source model. The reconstructions give for the ratio (theoretically 1) of biceps and brachialis activations 0.953 using the surface grid of 215 data and 0.91 using the 56 points on a ring.

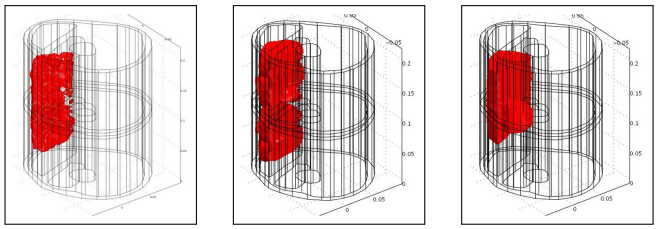

(a) Synthetic source model (b) Reconstructed model with surface data (215 points) (c) Reconstructed model with ring data (56 points)

Fig. 4. Results as in Fig. 3 with artificial sources placed in the biceps only. The reconstructions give for the ratio (theoretically 0) of brachialis and biceps activations 0.03 using the surface grid of 215 data and 0.05 using the 56 points on a ring.

subject applied an isometric extension and data was taken in the same fashion. This is expected to activate mainly the triceps but possibly also the other two muscles which provide stabilization during an isometric extension.

As we currently have no MRI data of our subject, we used the generic arm muscle model from [18], scaled to match the measured circumference (30cm) of the subject's arm at the location of the electrodes. A random sample of the middle 1 second of the data was chosen for the reconstruction. No significant difference was observed by the choice of sample. Besides the human data we also generated corresponding synthetic data with 5000 tripole sources. A coarse mesh of $32,607$ elements was used for the data inversion, whereas a finer mesh of $61,452$ elements was employed to generate synthetic measurement data, so as to avoid the so called "inverse crimes". For the artificial source modeling we use the simplest triangular model [2], with a pulse length of 1 cm. We observed no difference in results when the slightly more detailed Rosenfalck model [19] was substituted. If so desired more realistic models for the IAP

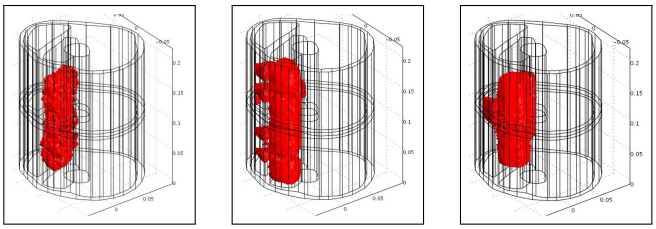

(a) Synthetic source model

(b) Reconstructed model with surface data (215 points)

(c) Reconstructed model with ring data (56 points)

Fig. 5. Results as in Fig. 3 and 4 with artificial sources placed in the brachialis only. The reconstructions give for the ratio (theoretically 0) of biceps and brachialis activations 0.11 using the surface grid of 215 data and 0.54 using the 56 points on a ring. In the ring configuration, 35% of the activity is erroneously attributed to the biceps instead of the brachialis, which indicate this sensor configuration is not adequate. As the brachialis is mostly covered by other muscles it is the hardest to identify.

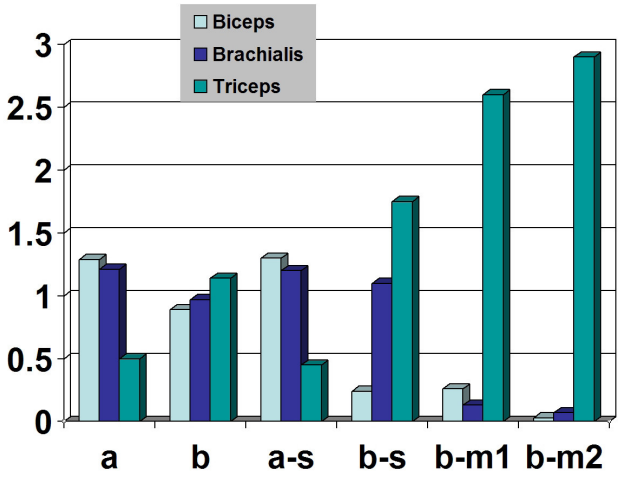

Fig. 6. Relative current source power densities in three muscles. Reconstructions were performed using human sEMG data during flexion (a) and extension (b). We used a generic morphometric model of the arm, scaled to match the circumference of the subject's arm. The results from (a) look plausible as the main activity is in the biceps and brachialis, as expected. The result (b) from isometric extension of the triceps seems to indicate a significant amount of coactivation of the biceps and brachialis, which is also plausible, as it is difficult not to activate these muscles for stabilization during the exercise. To check for consistency we generated synthetic data and corresponding reconstructions by placing 5000 simulated tripole sources in biceps and brachialis (a-s) and then just in the triceps (b-s). The synthetic result (a-s) is very close to the real result (a), but the synthetic results (b-s) which should show only activity in the triceps shows a significant amount of spurious coactivation in the brachialis, though not as much as in the real result (b). This is an indicator that this sensor configuration is inadequate to distinguish individual muscles accurately. To verify this hypothesis we computed synthetic data for a ring of 56 monopolar (b-m1) and for a surface grid of 215 monopolar sensors (b-m2) and it can be seen that the erroneous coactivation of the brachialis is no longer present.

(for example [2], [20]) could be employed, but since we use our sources only to test the inversion method there is no need for accuracy here. The sources were distributed over biceps and brachialis for the first exercise, and over the triceps for the second exercise. The results for the relative activations of the muscles are depicted in Fig. 6.

Discussion

We conclude that with this arrangement of bipolar sensors, while the activities of individual muscles can still be discriminated to some extent, significant "leaking" of reconstructed activity into nearby inactive muscles results in a low quality of the reconstruction. Experiments with synthetic data indicated that monopolar sensors will greatly improve the quality of the reconstruction, which is also to be expected on theoretical grounds. Another important conclusion we draw is that the results from synthetic and human data are consistent so we are confident that conclusions drawn from experiments with synthetic data are reliable and carry over to human data.

We found all reconstructions to be robust against uncertainties in the detailed properties such as conductivities and details of the geometry. Additional experiments (not reported here) were performed with values of conductivities in the reconstruction that differ by up to a factor of 2 from their "true" values (as used by the forward model) which still gave good reconstructions. This is important for practical purposes as the conductivities are not known to great accuracy [3].

IV. Conclusions

Our new CMG technique has the potential to greatly improve current practice in muscle function monitoring. Results from simulated experiments with synthetic data indicate that a surface grid of monopolar sEMG sensors, similar to configurations used in EEG, is to be preferred over the more commonly used bi- or tripolar voltage sensors. The results we obtained with human data using bipolar sensors are consistent with the results obtained from simulated data, even though the 3D arm model used for the analysis of human data was just a generic model. This suggests that simulated experiments are reliable indicators for the performance of the CMG system.

In the near future we plan to test the CMG system more extensively with human data from monopolar sensors. We will also acquire a more complete and patient specific 3D upper arm model from a set of cross sectional MR images at different elevations. The model used for our present results is based on an image of a single slice and is symmetric in the vertical axis.

To validate the results obtained from human data an independent measure of muscle activations is necessary to compare with the CMG predictions. Since we need the activations in the bulk of the muscles, a verification with multiple single unit needle EMG recordings would be very intrusive. Instead, we plan to use MRI to monitor exercise induced signal changes which are primarily due to an increase or decrease in the transverse relaxation time (T2) of tissue water [21], [22].

References

[1] A. Curt, M. Schwab, and V. Dietz, "Providing the clinical basis for new interventional therapies: refined diagnosis and assessment of recovery after spinal cord injury," *Spinal Cord*, vol. 42, pp. 1–6, 2004.

[2] R. Merletti and P. A. Parker, *Electromyography. Physiology, Engineering and Noninvasive Applications*. IEEE Press, John Wiley and Sons, 2004.

[3] M. M. Lowery, N. S. Stoykov, A. Taflove, and T. A. kuiken, "A Multiple-Layer Finite-Element Model of the Surface EMG Signal," *IEEE trans. on Biomedical Engineering*, vol. 49, no. 5, pp. 446–454, 2002.

[4] H. L. F. Helmholtz, "Ueber einige Gesetze der Verheilung elektrischer Ströme in körperlicher Leitern mit Anwendung auf die thierisch-elektrischen Versuche," *Ann. Physik und Chemie*, vol. 9, pp. 211–233, 1853.

[5] J. Stonick, R. Jesinger, V. Stonick, and S. Baumann, "Estimation and localization of multiple dipole sources fornoninvasive mapping of muscle activity," *IEEE International Conference on IEEE International Conference on Acoustics, Speech, and Signal Processing, ICASSP-96, Conference Proceedings*, vol. 5, pp. 2912–2915, 1996.

[6] R. LoPresti, E. F. andJesinger and V. Stonick, "Identifying Significant Frequencies in Surface EMG Signals for Localization of Muscle Activity," in *IEEE EMBS Conference Prodceedings*, 1995, pp. 967–968.

[7] R. Jesinger and V. Stonick, "Processing Signals from Surface Electrode Arrays for Noninvasive 3D Mapping of Muscle Activity," in *IEEE DSP Workshop Prodceedings*, 1994, pp. 57–60.

[8] E. Chauvet, O. Fokapu, and D. Gamet, "Inverse problem in the surface EMG: A feasibility study," in *Proceedings of the 23rd Annual EMBS international Conference, Istanbul, Turkey*, 2001, pp. 1048–1050.

[9] G. Drost, D. F. Stegeman, B. G. M. v. Engelen, and M. J. Zwarts, "Clinical applications of high-density surface emg: A systematic review," *Journal of Electromyography and Kinesiology*, vol. 16, pp. 586–602, 2006.

[10] B. G. Lapatki, I. E. Jonas, M. J. Zwarts, and D. F. Stegeman, "A thin, flexible multi-electrode grid for high-density surface EMG," *Journal of Applied Physiology*, vol. 96, pp. 327–336, 2004.

[11] C. J. De Luca, A. Adam, L. D. Gilmore, and S. H. Nawab, "Decomposition of Surface EMG Signals," *Journal of Neurophysiology*, vol. 96, pp. 1646–1657, 2006.

[12] J. M. Kilner, S. N. Baker, and R. N. Lemon, "A novel algorithm to remove electrical cross-talk between surface emg recordings and its applicaiton to the measurement of short term synchronization in humans," *The Journal of Physiology*, vol. 538, pp. 919–930, 2002.

[13] C. M. Michel, M. M. Murray, G. Lantz, S. Gonzalez, L. Spinelli, and R. G. d. Peralta, "Eeg source imaging," *Clinical neurophysiology*, vol. 115, pp. 2195–2222, 2004.

[14] R. D. Pascual-Marqui, "Standardized low resolution brain electromagnetic tomography (sLORETA): technical details," *Methods and Findings in Experimental and Clinical Pharmacology*, vol. 24D, pp. 5–12, 2002.

[15] H. W. Engl, M. Hanke, and A. Neubauer, *Regularization of Inverse Problems*. Kluwer, 1996.

[16] C. Vogel, *Computational methods for inverse problem*. Philadelphia: SIAM, 2002.

[17] K. van den Doel and U. Ascher, "Dynamic level set regularization for large distributed parameter estimation problems," *Inverse Problems*, vol. 23, pp. 1271–1288, 2007.

[18] H. Gray, *Henry Gray's Anatomy of the Human Body*. Yahoo online edition, 1858.

[19] P. Rosenfalck, "Intra- and extracellular potential fields of active nerve and muscle fibers: A physio-mathematical analysis of different methods," *Acta Physiol Scand*, vol. 321 (suppl, pp. 1–168, 1969.

[20] K. C. McGill and Z. C. lateva, "A Model ofthe Muscle-Fiber Intracellular Action Potential Waveform, Including the Slow Repolarization Phase," *IEEE Transactions on Biomedical Engineering*, vol. 48, no. 12, pp. 1480–1483, 2001.

[21] R. Kinugasa, Y. Kawakami, and T. Fukunaga, "Quantitave assessment of skeletal muscle activation using muscle functional MRI," *Magnetic Resonance Imaging*, vol. 24, pp. 639–644, 2006.

[22] S. B. Giodano and R. L. Segal, "Leg Muscles Differ in Spatial Activation Patterns with Differing Levels of Voluntary Plantarflexion Activity in Humans," *Cell Tissues Organs*, vol. 184, pp. 42–51, 2006.